Preparation and Characterization of Polyvinylpyrollidone Incorporated Cellulose Acetate Membranes for Ultrafiltration of Metal Ion

Archana Kumari, Gautam Sarkhel, Arup Choudhury

Department of Chemical and Polymer Engineering, Birla Institute of Technology, Mesra, Ranchi 835215, India

Received 4 March 2011; accepted 4 December 2011
DOI 10.1002/app.36616
Published online 26 January 2012 in Wiley Online Library (wileyonlinelibrary.com).

ABSTRACT: Cellulose acetate (CA) membranes are widely used for reverse osmosis and ultrafiltration (UF) applications. In this study, asymmetric CA membranes were prepared by phase inversion method using different concentration of polyvinylpyrollidone (PVP) as a pore former. The prepared polymeric blend membranes were characterized by Fourier transmission infrared spectroscopy, thermogravimetric analysis, and scanning electron microscope. The effect of PVP concentration on the UF performance of the blend membranes was investigated and discussed in terms of water content (%), compaction, and pure water flux (PWF). It was observed that the thermal stability of the membranes increased with increasing the PVP content, whereas the mechanical strength of membranes was deteriorated. The number of pore and pore size distribution in the membrane structure were evaluated. The PWF and water content (%) of the membranes were dependent on the PVP concentration. Studies were carried to find out the rejection and permeate flux of cadmium ion using humic acid as the chelating agent. © 2012 Wiley Periodicals, Inc. J Appl Polym Sci 124: E300–E308, 2012

Key words: cellulose acetate membrane; polyvinylpyrollidone; phase inversion; morphology; water flux; mechanical strength

INTRODUCTION

In recent years, membrane separation processes have attracted considerable interest in various potential applications such as water desalination, ultrapure water production, oil–water separation, production of beverages, electrocoat paint recovery, etc. Membrane separation processes are more important than other separation processes due to low-energy consumption, easy scale-up, less or no use of chemicals, and no harmful by-product formation.[1–4] The various membrane processes and range of particles diffusing through or retained are based on the membrane pore sizes. Membrane separation processes like microfiltration (MF), ultrafiltration (UF), reverse osmosis (RO), electrodialysis (ED), etc., are used in many industries for the recycling of rare metals, toxic chemicals, biomolecules, polymer binders, colloidal particles, etc.

UF is the most commonly used membrane separation method for separation of many desirable and undesirable components present in a solution. Many polymers such as cellulose acetate (CA), polyvinyl alcohol, polysulfones, polyethersulfones, polyacrylonitriles, polyvinylidenefluoride, and polyetherimides have been utilized to prepare asymmetric UF membranes through phase inversion method. CA has become a potential choice for aqueous-based separation, i.e., RO, MF, and UF techniques.[5–7] CA offers many advantages like high biocompatibility, good desalting, high-potential flux, and relatively low cost.[8–11] In addition, CA membranes have excellent hydrophilic character and consequently exhibit good fouling resistance for aqueous-based separation process, e.g., protein fouling.[12–14] However, CA is not suitable for more aggressive cleaning because of its poor mechanical strength, low oxidation, chemical resistances, and thermal instability.[15] Therefore, modification of CA membrane is an important aspect to avoid these problems and subsequently make it suitable for specific application.

In membrane technology, three different types of membrane modification techniques have been proposed: (i) membrane polymer modification (premodification), (ii) blending of the membrane polymer with a modifying agent (additive), and (iii) surface modification after membrane preparation (postmodification). The blend membranes have better permselectivity and permeability than that of membrane composed by the individual polymers. Furthermore, the pore size of membrane also plays an important role in its performance during phase inversion technique, and hence, the pore former plays a key role for

Correspondence to: A. Choudhury (arup@bitmesra.ac.in).
Contract grant sponsors: Department of Science and Technology, State Government of Jharkhand, India.

the formation of pore sizes in the asymmetric membranes. The concentration of pore former and its polarity will strongly influence the membrane characterization.[16,17] Many researchers have used various pore formers such as polyethylene glycol (PEG) and polyvinylpyrollidone (PVP) for structural modification of CA membrane. PVP is one of the good pore formers because of its excellent miscible with CA membrane and also exhibit good solubility in water as well as in many organic solvents. Xu et al.[18] studied the role of PVP or PEG as polymeric additive in the formation of asymmetric hollow fiber UF membranes with poly(vinyl chloride). They found that the addition of PVP or PEG as additives can increase the membrane porosity and enhance the permeation flux by changing the membrane morphology. Ma et al.[19] investigated the effect of different molecular weights of PEG as a pore former on the morphology and performance of polysulfone membranes. Zereshki et al.[20] studied the effect of poly(*N*-vinyl-2-pyrrolidone) on poly(lactic acid) blend membranes for separation of ethanol/ethyl-*tert-butyl*-ether mixtures by pervaporation. Saljoughi et al.[21] have investigated the effect of PVP concentration and coagulation bath temperature on the morphology and performance of CA membranes. The effect of incorporation of PEG 600 on the UF performance of the polysulfone/sulfonated poly (ether ether ketone) blend membranes was studied by Arthanareeswaran et al.[22]

The objective of this study was to enhance permeation performance of CA membrane by blending with a pore former, PVP. The PVP concentration in the membrane composition was optimized for increasing the antifouling properties and controlling the porosity level in the membrane. Different techniques like Fourier transmission infrared spectroscopy (FTIR), thermogravimetric analysis (TGA), and scanning electron microscope (SEM) were used to characterize the prepared CA–PVP blend membranes. The UF performance of these blend membranes was studied in terms of water content (%), compaction, pure water flux (PWF). This work would be helpful for selective heavy metal separation by controlling the membrane pore size and pore size distribution.

EXPERIMENTAL

Materials

CA (M_w = 61,000 g/mol, acetyl content of 40%) used as the membrane forming material, was received from CDH, India. PVP K30 (M_w = 40,000 g/mol) was procured from CDH, India, and used as a pore former. *N*,*N*-Dimethylformamide (DMF) was obtained from Central Drug House, India. Cadmium sulfate and humic acid (HA) were procured from Acros Organics, USA.

Preparation of CA membranes

Initially, CA was dried in vacuum oven at 100°C to remove the residual water from the polymer. The casting solutions were prepared by dissolving CA in DMF in the presence of PVP as a pore former of different concentrations (1, 2, and 3 wt %) under constant stirring for 4 h at 90°C. The solution was stand for 5 h for releasing air bubbles. The clear and homogeneous solution was cast on a clean and smooth glass plate using Doctor Blade. Then, the glass plate was immersed into deionized water coagulation bath (20°C). To accomplish complete phase separation, the membrane was kept in there for 12 h. After that the membrane was initially dried by placing it in between two blotting paper sheets at room temperature and finally, at 40°C under vacuum for 6 h. The dried membrane thickness was measured with a digital caliper device as 0.22 ± 0.02 mm.

Characterization

Fourier transmission infrared spectroscopy

FTIR spectra (attenuated total reflectance, ATR) were recorded on Shimadzu IR-Prestige 21 spectrophotometer in the spectral range of 650–4000 cm^{-1} with a resolution of 4 cm^{-1} at room temperature (23°C). Ten scans were taken for each membrane. Mercury cadmium telluride and potassium bromide were used as detector and beam-splitter, respectively.

Thermogravimetric analysis

The TGA was carried out in the DTG-60 (Shimadzu, Japan) thermal analyzer at the heating rate of 10°C/min under air atmosphere with a flow rate of 25 mL/min.

Morphological studies

The morphological characterization of the prepared membranes was performed using SEM (JEOL JSM-6390, Japan) at an acceleration voltage of 15 kV. The samples were sputtered with a thin layer of gold prior to SEM observation. In this study, "UTHSCSA" software was used to measure the pore size and pore size distribution for each formulated membrane. This software gives us the information regarding the number of pores in different pore size range, i.e., the pore size distribution from which percentage of pores in various pore size ranges was calculated. The mean pore radius, r_m (μm) is calculated as[23]

$$r_m = \frac{\sum n_i r_i^2}{\sum n_i} \quad (1)$$

where r_i is the radius of the pores and n_i is the number of pores of radius r_i. Assuming similar pore size

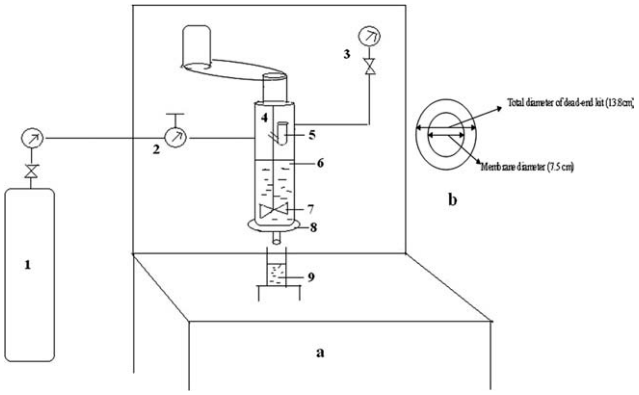

Figure 1 (a) Schematic diagram of UF test kit (1, compressed air; 2, inlet pressure valve; 3, outlet pressure valve; 4, UF test cell; 5, feed inlet; 6, feed tank; 7, stirrer; 8, membrane cell; 9, permeate) and (b) inner view of membrane cell.

distribution for the entire membrane sheet, the pore density, N (i.e., total number of pores per unit membrane area) is calculated using the following equation:

$$N(\mu m^2) = \frac{\sum n_i}{A_t} \quad (2)$$

where A_t is the total membrane area (μm^2) as calculated from the respective SEM image.

Mechanical stability

The mechanical properties of the different formulated membranes were determined by using Instron tensile testing machine (model 3366) with a crosshead speed of 50 mm/min and gripping length of 25 mm. The membrane films were cut into rectangle shaped strips with a dimension of 50 mm $\times$ 10 mm. At least five individual measurements were used to calculate the average values of mechanical properties.

Water content measurement

Membrane sample was dried in a vacuum oven and measured the initial weight of it with a high-precision balance. Then, it was soaked in water for 24 h followed by mopping with blotting paper and again weighed. The water content was calculated from the weight difference.[24]

$$\text{Water content}(\%) = \frac{\text{Wet sample weight} - \text{Dry sample weight}}{\text{Wet sample weight}} \times 100 \quad (3)$$

Pure water flux measurement

The flux experiment was carried out with an UF kit with an effective membrane surface area of 44.15 cm^2. The height of flow channel was 22.5 cm. The schematic diagram of UF kit is shown in Figure 1. The membranes were initially pressurized with deionized water for 5 h at a transmembrane pressure of 588.4 kPa. To monitor the compaction behavior till to achieve the steady flux, the PWF was repeatedly measured at 1-h interval. PWF experiments were conducted with prepressurized membrane at a transmembrane pressure of 490 kPa using the following equation:

$$J_w = \frac{Q}{A\Delta T} \quad (4)$$

where Q is permeating amount; A, membrane area; and ΔT, the sampling time.

Heavy metal separation studies

Aqueous solution of HA (0.03 g/L) and cadmium sulfate (0.205 g) was prepared and then used as feed solutions. Sodium chloride (0.01M) solution was used to adjust the ionic strength of the HA solution. The pH level of solution was maintained at 7 by adding 0.1M hydrochloric acid. After the membrane was mounted in the UF test kit, the chamber was filled with a known volume of cadmium solution and, measurements were operated at various pressures ranging from 196 kPa to 490 kPa. A constant agitation speed of 400 rpm was maintained throughout the study to reduce concentration polarization. The percent separation of cadmium ion was determined by analyzing the concentration of cadmium ions in the feed and the permeate streams by an inductively coupled plasma-optical emission spectroscopy (Perkin-Elmer Optima 2100 DV) and calculated by using eq. (5)

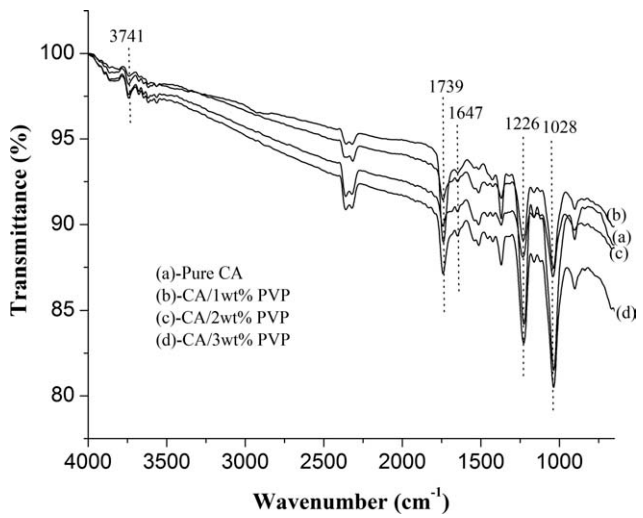

Figure 2 FTIR spectra of pure CA and different formulated CA–PVP blend membranes.

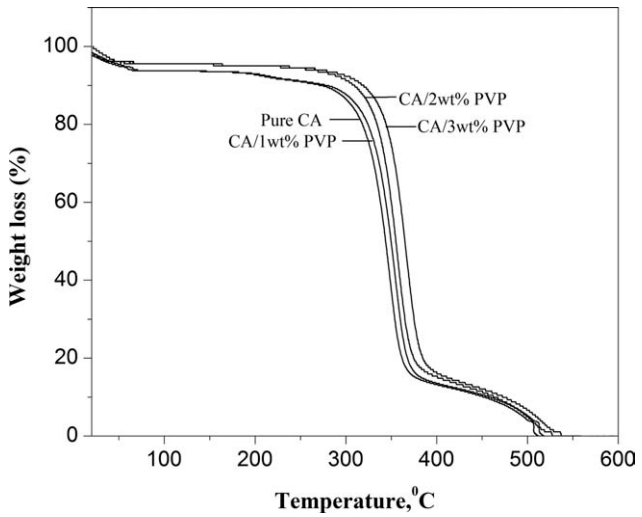

Figure 3 TGA curves of pure CA and different formulated CA–PVP blend membranes.

$$\text{Rejection}(\%) = \left(1 - \frac{C_p}{C_f}\right) \times 100 \quad (5)$$

where C_p and C_f are the concentration of permeate and feed solutions, respectively.

RESULTS AND DISCUSSION

FTIR studies

FTIR spectra of the pure CA membrane and the CA–PVP blend membranes are shown in Figure 2. The FTIR spectrum of pure CA membrane shows a broad absorption band at 3741 cm^{-1}, which is assigned to the stretching vibration of O—H. With increase of PVP content, the O—H absorption peak of the CA–PVP membranes became less pronounced with a shifting toward lower wavenumber (red-shift). This could be attributed to the formation of intermolecular hydrogen bonding between the O—H groups of CA and the C=O groups of PVP.[25] The peak located at 1739 cm^{-1} is assigned for the carbonyl stretching of CA and, two strong peaks at around 1231 and 1038 cm^{-1} are associated with the asymmetric and symmetric stretching vibration of the C—O—C bond. In comparison with FTIR spectrum of CA, the carbonyl band intensity is found to be decreased with after blending with PVP. This observation clearly suggests the intermolecular interaction between CA and PVP. In addition, the presence of a small peak at 1647 cm^{-1} is assigned to the amide carbonyl stretching of PVP component in the blend membrane.

TGA studies

The thermal degradation expressed in terms of weight loss as a function of the temperature for the pure CA and CA–PVP blend membranes were shown in Figure 3. The results of TG analysis are summarized in Table I. The small weight loss (~4%) below 90°C corresponds to the removal of residual solvent or moisture. The major decomposition is observed at the temperature range of 290–400°C for both pure CA and CA–PVP membranes. This is because the decomposition temperatures of both pure CA (~300°C) and PVP (~400°C) belong to this temperature range.[26,27] The onset temperatures of both first and second step thermal degradations are found to be remarkably higher in case of the CA–PVP membranes in comparison to pure CA (Table I). The increase in thermal stability of the CA–PVP membranes could be attributed to the strong intermolecular interaction via H-bonding between two polymer components.

Scanning electron microscope

Effect of pore former (PVP) on the CA membrane morphology was analyzed by SEM technique. SEM images of pure CA and different formulated CA–PVP membranes are shown in Figure 4. As shown in Figure 4, the number of pores and pore size are significantly increased by incorporation of PVP into CA. It indicates that PVP could be regarded as an efficient pore forming agent on the CA membrane. For CA–PVP membranes, the number of pore increased with increasing the concentration of PVP from 1 to 3 wt %, while pore size decreased with increase in PVP content. The presence of PVP increases

TABLE I
TGA Results of Pure CA and Different Formulated CA–PVP Membranes

	First-step degradation			Second-step degradation			
Membrane	Start temp. (°C)	End temp. (°C)	wt % loss	Start temp. (°C)	End temp. (°C)	wt % loss	Residue (wt %)
Pure CA	292	364	65.45	364	510	14.59	1.9
CA/1 wt % PVP	300	372	64.05	372	518	13.33	1.6
CA/2 wt % PVP	318	380	69.62	380	527	15.65	1.2
CA/3 wt % PVP	330	397	70.59	391	540	16.75	0.8

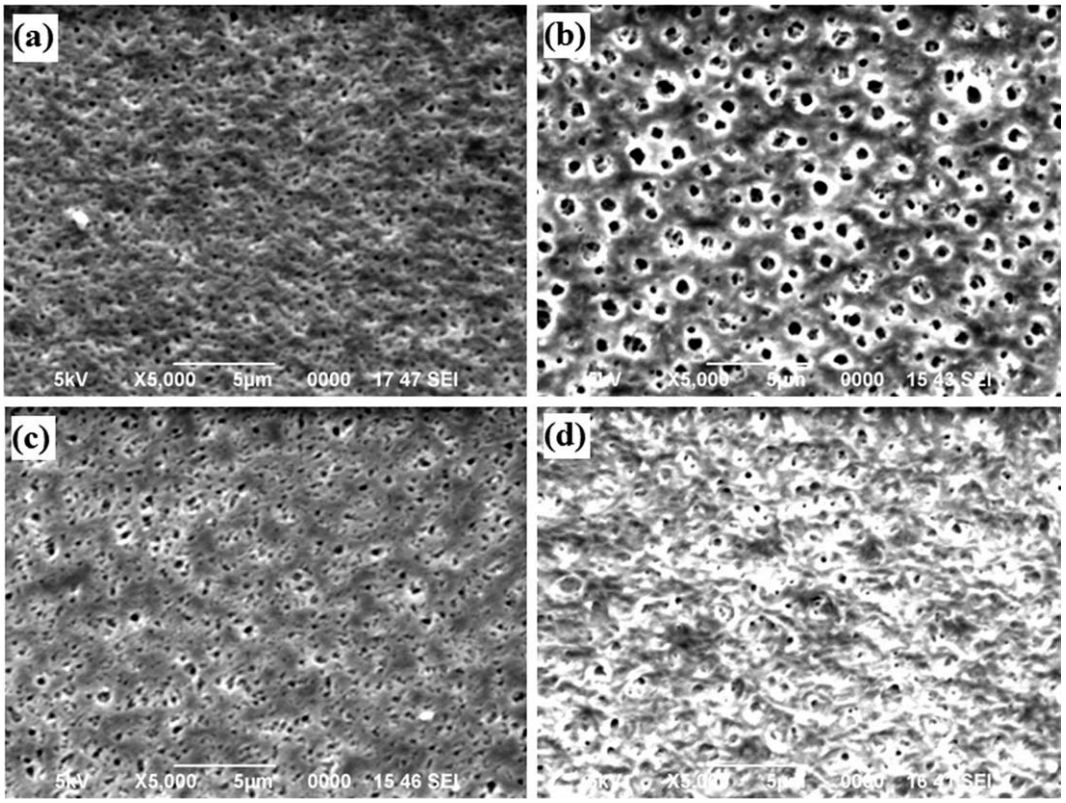

Figure 4 SEM micrographs of (a) pure CA membrane and CA–PVP blend membranes with PVP concentration of (b) 1, (c) 2, and (d) 3 wt %.

thermodynamic instability of the cast membrane and consequently leads to instantaneous demixing in the coagulation bath and thus, formation of macrovoids in the membrane structure.[28,29] Figure 4(b–d) depicts the porous layer with a uniform pore size distribution on the surface of CA–PVP blend membranes, indicating good miscibility between CA and PVP.

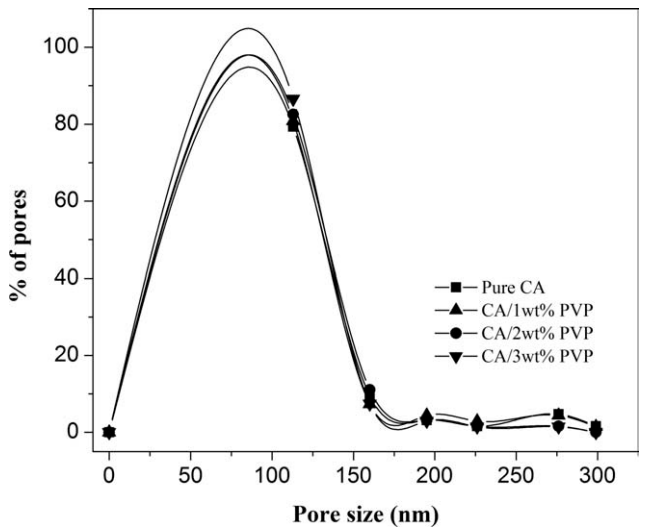

Figure 5 Pore size distribution of CA–PVP membranes with different PVP concentrations.

Pore statistics

Pore statistics such as pore size distribution, mean pore size, pore density, and porosity of different formulated membranes were determined by using the UTHSCSA software assuming the shapes of the pores to be circular. Figure 5 demonstrates the pore size distributions of all formulated CA–PVP membranes. The mean pore radii was calculated by using eq. (1)[23] for all membrane samples, given in Table II. As observed from Table II that the mean pore radius on pure CA membrane is recorded 0.1 μm, which reduced to 0.07 by addition of 3 wt % PVP. The pore density on the CA–PVP membrane is increased from 0.34 to 0.51 as the PVP concentration increase from 0 to 3 wt %.

TABLE II
Pore Statistics Properties of Prepared CA Membranes with Different Concentrations of PVP Obtained from SEM Analysis

Membrane	Mean pore radius (μm)	Pore density ($N/\mu m^2$)
Pure CA	0.10	0.34
CA/1 wt % PVP	0.14	0.40
CA/2 wt % PVP	0.09	0.48
CA/3 wt % PVP	0.07	0.51

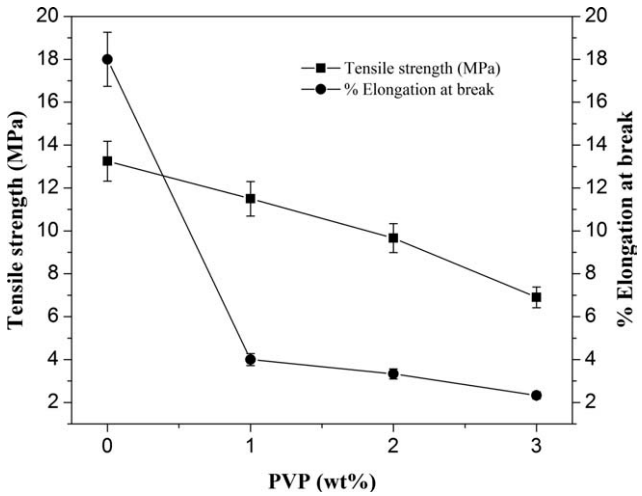

Figure 6 Variation of tensile strength and percent elongation at break of CA–PVP blend membrane as function of PVP concentration.

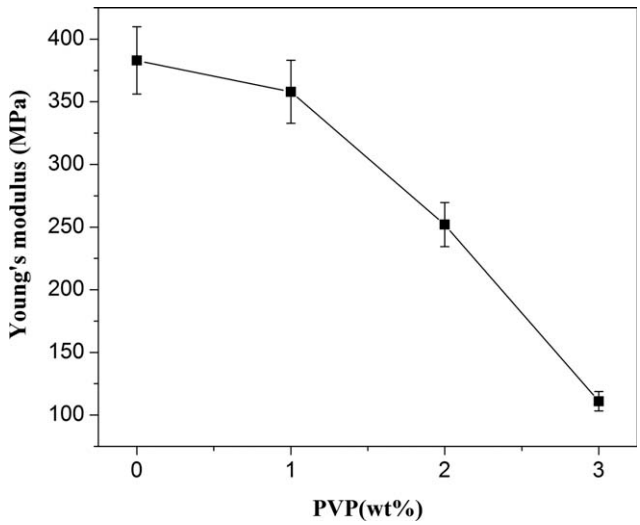

Figure 7 Variation of Young's modulus of CA–PVP blend membranes as a function of PVP concentration.

Mechanical properties

The mechanical properties such tensile strength, Young's modulus, and percent elongation at break of the pure CA and formulated CA–PVP membranes were measured, and results are demonstrated in Figures 6 and 7. It can be seen from those figures that the overall mechanical properties, particularly tensile strength and modulus, of CA were decreased by addition of PVP. For pure CA membrane, the values of tensile strength, Young's modulus, and percent elongation at break are recorded 13.25 MPa, 383 MPa, and 18%, respectively. Whereas the CA–PVP blend membrane with a PVP content of 3 wt % exhibited lower mechanical properties with a tensile strength of 6.9 MPa and Young's modulus of 111 MPa. This decreasing tendency of mechanical properties might be due to the fact that the incorporation of PVP at a lower content decreased the mobility of the CA chains and consequently weakened the mechanical strength of the blend membranes. The decrease in mechanical properties is also anticipated the formation of defects in terms of macrovoids or pores in the CA–PVP membranes.

Water content (%)

Water content is an important parameter for predicting the PWF behavior of the membrane. It is well correlated with the hydrophilicity and porosity of the membrane. The effect of concentration of pore former, PVP, on the water content of CA–PVP blend membranes is illustrated in Figure 8. The water content of pure CA membrane is recorded 70%, which is increased from 71.95 to 75.63% as the PVP concentration raises from 1 to 3 wt %. Hence, the incorporation of PVP significantly enhanced the water absorption capability. The increase in PVP content in blend might favor the formation of larger pores or cavities in the membrane, which are responsible for accommodating water molecules in the membranes and hence, increase the water content. Furthermore, the hydrophilic character of the PVP macromolecules could also promote the water absorption of the blend membranes.

Effect of compaction time on PWF

Compaction is an important parameter, which reflects the tolerance of membrane towards hydraulic pressure. This would be more useful, to apply the membrane for a particular environment and to identify the suitability of the membranes for a particular membrane process.[30,31] The effect of compaction

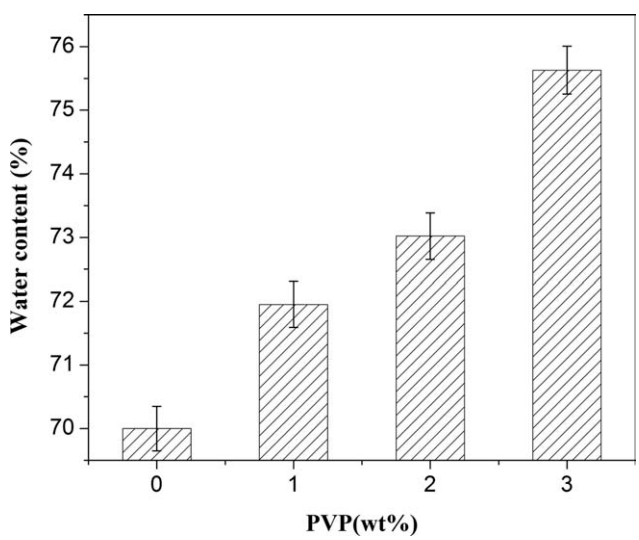

Figure 8 Effect of PVP concentration on water content for CA–PVP blend membranes.

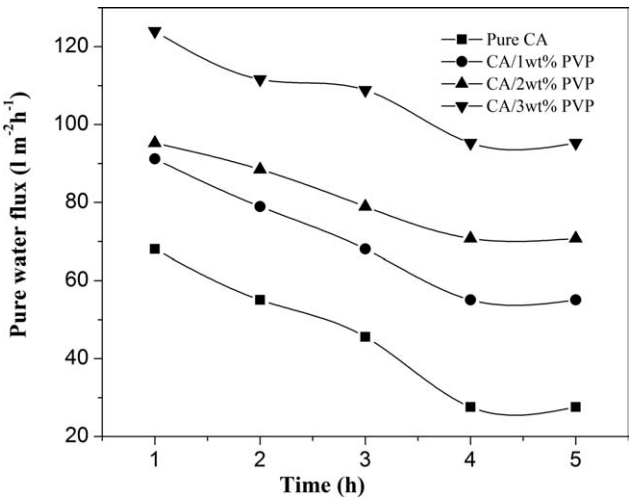

Figure 9 Variation of PWF as function of compaction time for CA–PVP blend membranes.

time on PWF for all the membranes is shown in Figure 9. PWF of the membranes were evaluated for every 1 h at constant operating pressure (i.e., 490 kPa). For all the types of membranes, the PWF is seen to slowly decrease with time due to compaction and finally attain a steady state after 4 h of compaction (Fig. 9). This is due to the fact that during compaction of polymeric membrane under hydraulic pressure, the walls of the pores become closer, denser, and uniform resulting in reduction in pore size as well as the flux.[32] The pure CA membrane exhibited an initial water flux of 68.05 L m^{-2} h^{-1}, which decreased to a steady state value of 27.54 L m^{-2} h^{-1} after 4-h compaction. An increase in PVP concentration to 1 wt % enhanced the water flux of CA membrane from 27.54 to 55.12 and finally to 95.26 L m^{-2} h^{-1} at 3 wt % PVP. It can also be noticed from the figure that the steady state PWF increases with increase in PVP content. The increase in flux in presence of PVP might be due to the fact that PVP acts as a nonsolvent swelling agent, thereby generating more extensive network pores in the membrane.[33]

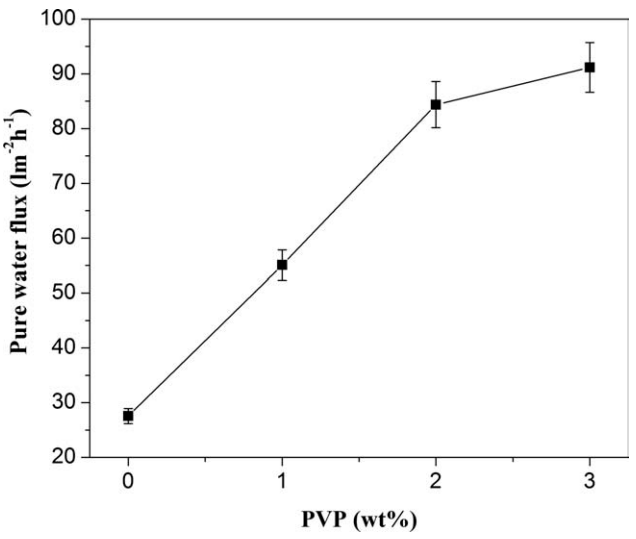

Figure 10 Effect of PVP concentration on PWF of CA–PVP blend membranes.

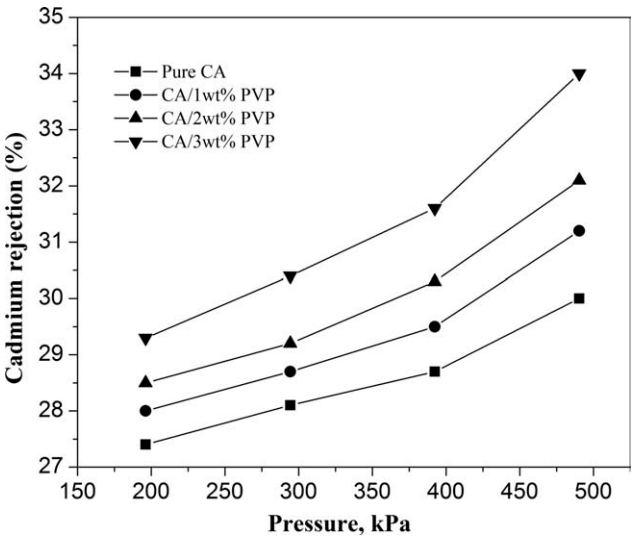

Figure 11 Effect of applied pressure on cadmium rejection (%) of CA–PVP blend membrane.

Effect of PVP concentration on PWF

The effect of PVP concentration on PWF of the CA–PVP blend membranes at equilibrium is shown in Figure 10. The PWF of pure CA membrane is recorded 27.54 L m^{-2} h^{-1}. The PWF of CA–PVP blend membrane is found to increase from 55.1 to 91.18 L m^{-2} h^{-1} as PVP content increase from 1 to 3 wt %. However, as PVP content increase beyond 2 wt %, the increase in flux is relatively smaller than that observed below 2 wt % PVP. The increase PWF with PVP content could be explained from the fact that increase in concentration of PVP has resulted in a membrane with a highly porous substructure due to the presence higher number of macrovoids, which leads to higher flux. This fact can also be understood from the SEM images (Fig. 4).

Heavy metal separation studies

The pH value is one of the most important factors in the interaction of a metal ion with a binding polymer.[34–36] Heavy metals exist as free ions in a strong acidic medium. At this condition, metal ions could freely pass through the UF membrane because of their molecular sizes are less than the pore sizes of the membrane. Hence, to enhance the size and subsequent rejection of metal ions, HA (chelating agent) was used to complex the cadmium ions. In this study, pH of the solution was adjusted to 8 ± 0.37

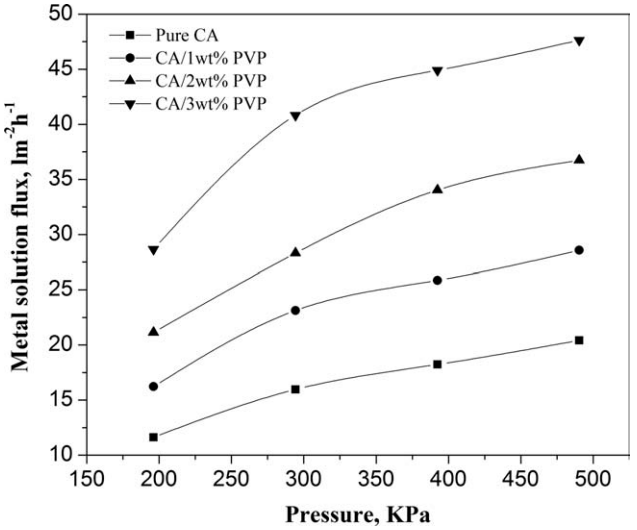

Figure 12 Effect of applied pressure on permeate flux of CA–PVP blend membrane.

for creating higher binding of cadmium ions with HA and thus, formation of hydroxo/aqua/complexes of metals.[37]

The effect of operation pressure on the percentage rejection of cadmium ions for the pure CA and CA–PVP blend membranes is shown Figure 11. It can be seen from Figure 11 that the rejection of Cd^{2+} ions increased with increasing operation pressure for all type membranes. Pure CA membrane offered rejection value of 27.4% at 196 kPa, which increased to 30.2% at 490 kPa. However, for CA–PVP blend membrane containing 3 wt % PVP, the rejection increases from 29.3 to 34.4% as the operation pressure increase from 196 to 490 kPa. The possible reason is that when the operation pressure increase, the ion transport due to convection becomes predominant compared to diffusion. It can also be seen from Figure 11 that at constant pressure, the percent rejection of Cd^{2+} ions is increased upon increasing the concentration of PVP in the blend membrane. At 1 wt % PVP content, percent rejection is recorded 31.2% (490 kPa) and then, it increased to 34.4% (490 kPa) as PVP concentration increase to 3 wt %. This increasing trend in rejection was due to the fact that the pore size of the membranes is decreased as the concentration of PVP (1–3 wt %) in the membrane casting solution increased. Figure 12 presents the variation of flux as a function of operation pressure. The permeate flux increases linearly with increasing operation pressure, which suggests that there may be negligible concentration polarization in the membrane cell.[38] However, the permeate flux observed for pure CA membrane is significantly improved by blending with PVP. For instance, the flux for pure CA membrane is recorded 20.41 L m^{-2} h^{-1} at 490 kPa, which is enhanced to 47.63 L m^{-2} h^{-1} for CA–PVP blend membrane containing 3 wt % PVP. From these results, it is understood that the rejection and flux characteristics of the membrane strongly depend on the structure of the membrane. The variation in morphological structure of the membrane due to blending of PVP of different concentration is an important factor in Cd^{2+} ions rejection.

CONCLUSIONS

In the present investigation, various CA–PVP blend membranes with different PVP concentrations were prepared and their morphology and PWF were evaluated. The FTIR spectroscopic results indicated the presence of interaction between CA and pore-forming agent (PVP) via a hydrogen bond. SEM photographs showed that PVP pore former played a crucial role in modifying the structure of membranes with higher porosity. With increase in the concentration of PVP, pore size is decreased but pore density and porosity of membranes are increased. It was found that the PVP concentration have major influence on the UF characteristics of blend membranes such as compaction, PWF and water content. The water flux value of CA control membrane is recorded only 27.54 L m^{-2} h^{-1}; however, it dramatically increased to 91.18 L m^{-2} h^{-1} when PVP content in the blend membrane reached 3 wt %. Both the rejection (%) and permeate flux of cadmium ion is increased with increasing applied pressure. The results presented here would be extended to the commercial purpose and industrial applications.

References

1. Peng Suna, S.; Yu Wang, K.; Peng, N.; Alan Hattona, T.; Chunga, T. S. J Membr Sci 2010, 363, 232.
2. Noble, R. D.; Stern, S. A. Membrane Separation Technology, Principles and Applications; Elesvier Science, Amsterdam, The Netherlands, 1995.
3. Yu, S.; Liu, M.; Ma, M.; Qi, M.; Lu, Z.; Gao, C. J Membr Sci 2010, 350, 83.
4. Cassano, A.; Molinari, R.; Romano, M.; Drioli, E. J Membr Sci 2001, 181, 111.
5. Qin, J. J.; Oo, M. H.; Cao, Y. M.; Lee, L. S. Sep Purif Technol 2005, 42, 291.
6. Qin, J. J.; Li, Y.; Lee, L. S.; Lee, H. J Membr Sci 2003, 218, 173.
7. Arthanareeswaran, G.; Sriyamuna Devi, T. K.; Raajenthiren, M. Sep Purif Technol 2008, 64, 38.
8. Idris, A.; Yet, L. K. J Membr Sci 2006, 280, 920.
9. Hayama, M.; Yamamoto, K.; Kohori, F.; Sakai, K. J Membr Sci 2004, 234, 41.
10. Dunweg, G.; Lother, S.; Wolfgang, A. US Pat 1995, 540, 3485.
11. Ferjani, E.; Lajimi, R. H.; Deratani, A. Desalination 2002, 146, 325.
12. Majewska-Nowak, K.; Kowalska, I.; Kabsch-Korbutowicz, M. Desalination 2005, 184, 415.
13. Zularisam, A. W.; Ismaila, A. F.; Salimc, M. R.; Sakinaha, M.; Ozakid, H. Desalination 2007, 212, 191.
14. Ramírez, J. A. L.; Oviedo, M. D. C.; Alonso, J. M. Q. Desalination 2006, 191, 137.
15. Arthanareeswaran, G.; Thanikaivelan, P.; Srinivasn, K.; Mohan, D.; Rajendran, M. Eur Polym J 2004, 40, 2153.

16. Kesting, R. E. Synthetic Polymeric Membranes—A Structural Perspective; Wiley-Inter Science: New York, 1985.
17. Wu, H.; Fang, X.; Zhang, X.; Jiang, Z.; Li, B.; Ma, X. Sep Purif Technol 2008, 64, 183.
18. Xu, J.; Xu, Z. L. J Membr Sci 2002, 208, 203.
19. Ma, Y.; Shi, F.; Ma, J.; Wu, M.; Zhang, J.; Gao, C. Desalination 2011, 272, 51.
20. Zereshkia, S.; Figoli, A.; Madaeni, S. S.; Galiano, F.; Drioli, E. J Membr Sci 2011, 373, 29.
21. Saljoughi, E.; Mohammadi, T. Desalination 2009, 249, 850.
22. Arthanareeswaran, G.; Mohan, D.; Raajenthiren, M. J Membr Sci 2010, 350, 130.
23. Chakrabarty, B.; Ghoshal, A. K.; Purkait M. K. J Coll Interface Sci 2008, 320, 245.
24. Sivakumar, M.; Mohansundaram, A. K.; Mohan, D.; Balu, K.; Rangarajan, R. J Appl Polym Sci 1998, 67, 1939.
25. Miyashita, Y.; Suzuki, T.; Nishio, Y. Cellulose 2002, 9, 215.
26. Chatterjee, P. K. J Polym Sci 1968, 6, 3217.
27. Lucena, M. C.; Alencar, A. E. V.; Mazzeto, S. E.; Soares, S. A. Polym Degrad Stab 2003, 80, 149.
28. Kim, I. C.; Lee, K. H. J Membr Sci 2004, 230, 183.
29. Malaisamy, R.; Mahendran, R.; Mohan, D.; Rajendran, M.; Mohan, V. J Appl Polym Sci 2002, 86, 1749.
30. Reinsch, V. E.; Greenberg, A. R.; Kelley, S. S.; Peterson, R.; Bond, L. J. J Membr Sci 2000, 171, 217.
31. Brinkert, L.; Abidine, N.; Aptel, P. J Membr Sci 1993, 77, 123.
32. Mulder, M. Basic Principles of Membrane Technology; Kluwer Academic Publishers: Dordrecht, 1991.
33. Jian-Jun, Q. Fook-Sin, Ying, W. L. Yu-Tie, L. J Membr Sci 2003, 211, 139.
34. Juang, R. S.; Chiou, C. H. J Membr Sci 2000, 177, 207.
35. Muslehiddinoglu, J.; Uludag, Y.; Ozbelge, H. O.; Yilmaz, L. J Membr Sci 1998, 140, 251.
36. Zeng, J.; Ye, H.; Hu, Z. J Hazard Mater 2009, 161, 1491.
37. Alpatova, A.; Verbych, S.; Bryk, M.; Nigmatullin, R.; Hilal, N. Sep Purif Technol 2004, 40, 155.
38. Vidya, S.; Vijayalakshmi, A.; Nagendran, A.; Mohan, D. Sep Sci Technol 2008, 43, 1933.